Oscillation-Induced Layer-by-Layer Electrodeposition Producing Alternate Metal and Metal-Alloy Multilayers on a Nanometer Scale

Sho-ichiro Sakai, Shuji Nakanishi, Kazuhiro Fukami, and Yoshihiro Nakato*
Department of Chemistry, Graduate School of Engineering Science, Osaka University, Toyonaka, Osaka 560-8531

(Received March 25, 2002; CL-020266)

A current oscillation appears in electrodeposition of Cu and Sn in an acidic solution containing a cationic surfactant. The oscillation leads to layer-by-layer deposition producing alternate metal and metal-alloy multilayers on a nanometer scale.

Structurally regulated electrodeposition of metals and semiconductors by coupling with electrochemical oscillations is an interesting target from the point of view of production of micro- and nano-structured materials. In 1989, Krastev et al. reported[1] that the codeposition of Sb and Ag showed a current oscillation, giving layered deposits with target patterns of a micrometer size at the surface. The interesting result was later reproduced and developed by Nakabayashi et al.[2] Recently Switzer et al. reported[3] that the electrodeposition of Cu in neutral aqueous solutions caused a current oscillation, producing alternate Cu and Cu_2O multilayers on a nanometer scale. Unfortunately, in both cases, no mechanisms have been revealed yet. In the present paper, we report a new mechanism for oscillation-induced layer-by-layer electrodeposition, which was revealed through studies on a current oscillation appearing in the deposition of Cu and Sn, first reported by Survila et al.[4]

Polycrystalline discs of Cu, Sn and Au (99.99%), about 6.0 mm in diameter, were used as the working electrode, together with a $10 \times 10\,mm^2$ Pt plate as the counter electrode and an Ag/AgCl/saturated-KCl electrode as the reference electrode. The metal disc electrodes were polished with diamond slurry and immersed in hot 1.5 M HNO_3 + 1.5 M H_2O_2 for 10 min to remove surface contamination. The electrolyte was 0.6 M H_2SO_4 containing Cu^{2+}, Sn^{2+}, or both. A surfactant, N,N-bis(decaoxyethylene)octadecylamine, called Amiet-320 (KAO Corp.), was in some cases added to the electrolyte. Current density (j) vs potential (U), and j vs time (t) were recorded digitally at 1 kHz with a data-storing system (instruNET, GW Instruments). The electrode surface was inspected with a Hitachi S-5000 high-resolution scanning electron microscope (SEM).

Figure 1 shows j vs U for (A) Sn deposition, (B) Cu deposition, and (C and C′) Cu and Sn codeposition, all obtained in the first negative potential scans. An inlet (A′) is an expansion of (A) in the region of current onsets. The Sn deposition on Sn starts to occur at about −0.45 V (curve a), whereas that on a Cu electrode starts at a slightly more positive potential of about −0.35 V (curve b). The Cu deposition on Cu starts at a much more positive potential of about +0.05 V (curve d).

It is to be noted that the Sn deposition on Sn in the presence of Amiet-320 shows a negative differential resistance (NDR), designated as NDR-1 (curve c), whereas the Cu deposition on Cu shows no NDR even in the presence of Amiet-320 (curve e). Interestingly, the codeposition of Cu and Sn shows another NDR, designated as NDR-2, in the presence of Amiet-320 (curves i ∼ k). In the potential regions of both NDR-1 and NDR-2, current oscillations appear when a resistance is added to the external circuit. Figure 2 shows j vs t for a current oscillation at −0.41 V (in the region of NDR-2) with an external resistance of 3.5 Ω.

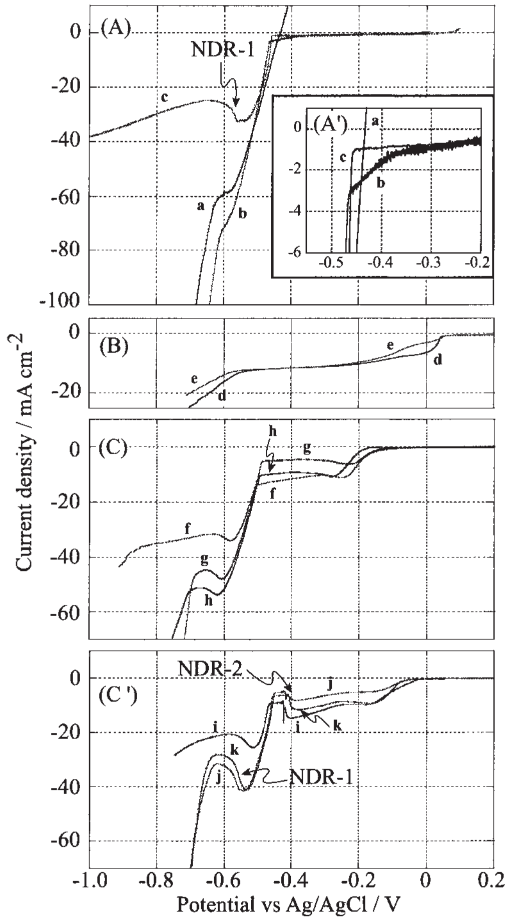

Figure 1. j vs U for (A and A′) Sn deposition, (B) Cu deposition, and (C and C′) Cu and Sn codeposition. Electrolyte: 0.6 M H_2SO_4 containing (curves a ∼ c) 0.3 M $SnSO_4$, (curves d ∼ e) 0.1 M $CuSO_4$, (curves f and i) 0.15 M $SnSO_4$ + 0.1 M $CuSO_4$, (curves g and j) 0.3 M $SnSO_4$ + 0.05 M $CuSO_4$, and (curves h and k) 0.3 M $SnSO_4$ + 0.1 M $CuSO_4$. In addition, 0.5 and 0.3 mM Amiet-320 are added for curve c and curves e, i, j, k, respectively. Electrode: Au, except for Sn for curve a and Cu for curves b and c.

Let us hereafter focus our attention on NDR-2 and the corresponding oscillation. The nearly potential-independent current in −0.2 to −0.5 V in Figure 1(C) is in proportion to the Cu^{2+} concentration (curves g and h), indicating that the current is mainly due to the Cu deposition. NDR-2 in Figure 1(C′) starts to appear at a potential at which the Sn deposition on Cu starts (curve

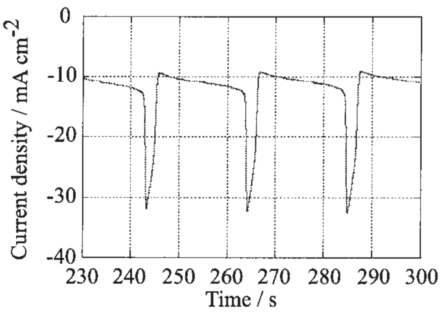

Figure 2. j vs t at -0.41 V with an external resistance of 3.5 Ω. Electrolyte: 0.3 M $SnSO_4$ + 0.1 M $CuSO_4$ + 0.6 M H_2SO_4+ 0.3 mM Amiet-320.

b in (A′)), indicating that the codeposition of Sn and Cu, though the Cu deposition is still dominant, causes the appearance of NDR-2. Another important fact is that NDR-2 appears only in the presence of Amiet-320, as can be seen from comparison of (C) and (C′).

The appearance of NDR-2 can thus be explained as follows. The codeposition of Sn and Cu, in which the Cu deposition is dominant, should result in a negatively polarized surface, as schematically shown in Figure 3(A), owing to a difference in the electronegativity (or work function) between Cu and Sn as well as the principle of the equal Fermi level of electrons within a conductor. The negatively polarized surface induces the adsorption of Amiet-320 that is protonated and positively charged in 0.6 M H_2SO_4, which in turn retards the diffusion of Cu^{2+} and Sn^{2+} ions and causes a decrease in j. Such a decrease in j will start near the potential at which the Sn deposition on Cu starts and become stronger with negative potential shift, thus causing the appearance of NDR-2.

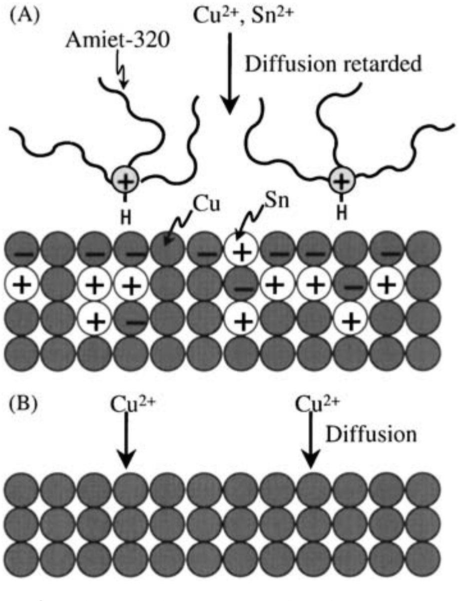

Figure 3. Schematic illustrations of surface structures and processes for (A) low-current and (B) high current states of the oscillation of Figure 2.

Next let us consider the current oscillation, for which U is kept constant in the potential region of NDR-2 (Figure 2). In a state of high current (in the absolute value), the true electrode potential E is considerably more positive than U, because E is given by $E = U - jAR$ where jAR is the ohmic drop between the working and the reference electrode (A is the electrode area, R the sum of the solution and external resistances, and j is negative for the reduction current). In other words, E is more positive than the potential region of NDR-2, and thus efficient Cu deposition proceeds with no adsorption of Amiet-320 (Figure 3(B)). The efficient Cu deposition, however, causes a decrease in the surface Cu^{2+} concentration owing to slow diffusion of Cu^{2+}, which in turn leads to a decrease in j and a negative shift in E. When E shifts to the negative and enters into the potential region of NDR-2, the codeposition of Sn and Cu starts, accompanied by the adsorption of Amiet-320, as mentioned earlier, which leads to a further decrease in j. Here is a positive feedback mechanism. Thus the electrode suddenly transfers from a high-current state to a low-current state.

In a low-current state, in which only slow deposition of Cu and Sn proceeds, the initially low surface Cu^{2+} concentration gradually increases again with time by diffusion, leading to a gradual increase in j and hence a gradual positive shift in E. The positive shift in E leads to a decrease in the Sn content of the Sn-Cu alloy (curve b in (A′)) and thus a decrease in the surface negative charge, which in turn leads to a decrease in the amount of adsorbed Amiet-320 and an increase in j. Here is also a positive feedback mechanism, causing a sudden inverse transfer from a low- to a high-current state.

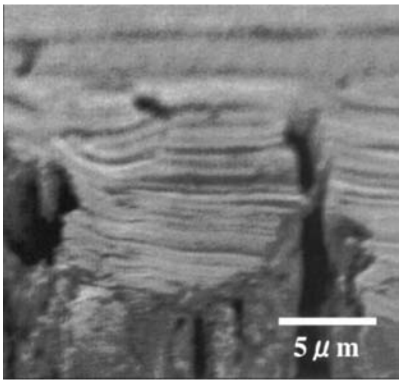

Figure 4. Cross-sectional SEM image of an electrodeposit, obtained after slight etching in 0.1 M HCl to make the image contrast sharper by selective dissolution of Sn in the Cu-Sn alloy layer.

It is to be noted that only Cu metal is deposited in the high-current state, whereas Cu-Sn alloy is deposited in the low-current state, and thus the current oscillation leads to layer-by-layer deposition producing alternate Cu and Cu-Sn multilayers. This expectation was actually confirmed by SEM inspection showing the formation of a multi-layered structure in the electrodeposits (Figure 4). The new mechanism revealed in the present work can be extended to various electrodeposition systems.

References

1 I. Krastev, M. Nikoklova, and I. Nakada, *Electrochim. Acta*, **34**, 1211 (1989).
2 S. Nakabayashi, I. Krastev, R. Aogaki, and K. Inokuma, *Chem. Phys. Lett.*, **294**, 204 (1998).
3 J. A. Switzer, C. J. Hung, L. Y. Huang, E. R. Switzer, D. R. Kammler, T. D. Golden, and E. W. Bohannan, *J. Am. Chem. Soc.*, **120**, 3530 (1998).
4 A. Survila, Z. Mockus, and R. Juskenas, *Electrochim. Acta*, **43**, 909 (1998).